Published in final edited form as:
J Cereb Blood Flow Metab. 2002 July ; 22(7): 890–898. doi:10.1097/00004647-200207000-00014.

[2,4-$^{13}C_2$]-β-Hydroxybutyrate Metabolism in Human Brain

Jullie W. Pan[*], **Robin A. de Graaf**[†], **Kitt F. Petersen**[†], **Gerald I. Shulman**[†], **Hoby P. Hetherington**[*], and **Douglas L. Rothman**[†]

[*]Albert Einstein College of Medicine, Bronx, New York

[†]Yale University School of Medicine, New Haven, Connecticut, U.S.A.

Summary

Infusions of [2,4-$^{13}C_2$]-β-hydroxybutyrate and ^{1}H–^{13}C polarization transfer spectroscopy were used in normal human subjects to detect the entry and metabolism of β-hydroxybutyrate in the brain. During the 2-hour infusion study, ^{13}C label was detectable in the β-hydroxybutyrate resonance positions and in the amino acid pools of glutamate, glutamine, and aspartate. With a plasma concentration of 2.25 ± 0.24 mmol/L (four volunteers), the apparent tissue β-hydroxybutyrate concentration reached 0.18 ± 0.06 mmol/L during the last 20 minutes of the study. The relative fractional enrichment of ^{13}C-4-glutamate labeling was 6.78 ± 1.71%, whereas ^{13}C-4-glutamine was 5.68 ± 1.84%. Steady-state modeling of the ^{13}C label distribution in glutamate and glutamine suggests that, under these conditions, the consumption of the β-hydroxybutyrate is predominantly neuronal, used at a rate of 0.032 ± 0.009 mmol · kg^{-1} · min^{-1}, and accounts for 6.4 ± 1.6% of total acetyl coenzyme A oxidation. These results are consistent with minimal accumulation of cerebral ketones with rapid utilization, implying blood–brain barrier control of ketone oxidation in the nonfasted adult human brain.

Keywords

Ketones; Magnetic resonance spectroscopy; ^{13}C; β-Hydroxybutyrate; Glutamate; Metabolism

Although glucose is the predominant fuel for the mammalian brain, it is well known that ketones can also be readily utilized, particularly under situations of fasting, strenuous exercise, or particular diets (Robinson and Williamson, 1980). In rodents, the measurement of the ketone contribution towards brain metabolism has typically been performed through extract or autoradiographic studies of radioactive tracers (Cremer, 1971; Nehlig et al., 1991). In studies of lightly anesthetized rodents, brain ketone consumption has been reported to be small, at approximately 3% of total (Hawkins et al., 1986). This contrasts to measurements made in humans, performed through [^{11}C]-β-hydroxybutyrate (BHB) positron emission tomography (PET) (Blomqvist et al., 1995) and AV difference measurements (Owen et al., 1965; Hasselbalch et al., 1994, 1996). In fasted and nonfasted human studies, ketones have been reported to provide a substantially larger fraction of brain oxidative metabolism, up to 50% of energy production in 3-week fasted obese subjects. The basis for these differences may have a variety of causes, including level of anesthesia, species differences, and physiologic state. In particular, entry of ketones has been shown by several investigators to be induced with fasting (Gjedde and Crone, 1975; Pollay and Stevens, 1980). Methodology may also contribute to variability; owing to intrinsic difficulties in assessing *in vivo* human

Address correspondence and reprint requests to J. W. Pan, Department of Neurology and Neuroscience, Albert Einstein College of Medicine, 1300 Morris Park Avenue, Bronx, NY 10461, U.S.A.; jpan@aecom.yu.edu .

brain metabolism, and the lack of a stable radiotracer for ketones, there has been little direct evidence for acute ketone use by the human brain.

Human brain metabolism may be also studied by carbon 13 (^{13}C) magnetic resonance (MR) spectroscopy. The ^{13}C nucleus is a stable isotope of carbon, which is nuclear magnetic resonance (NMR) detectable, and is naturally present at 1.1% abundance. The level of ^{13}C in brain metabolite pools may be measured regionally and noninvasively by localized ^{13}C or ^{1}H–^{13}C MR spectroscopy. As has been discussed by earlier papers using ^{13}C-labeled glucose (Rothman et al., 1992), the appearance of the ^{13}C into the amino acid pools can be modeled to determine the fraction of oxidative metabolism contributed by the labeled substrate. Additionally, determining the relative labeling of the glutamate, glutamine, and aspartate pools potentially allows the analysis of the metabolic and neurotransmitter cycling that occurs within neurons and glia.

The use of BHB to track cerebral metabolism should be clearer to interpret because, unlike glucose, BHB does not directly enter into the pyruvate carboxylase and the pyruvate dehydrogenase fluxes. Thus the metabolic flux of BHB should provide a more direct assessment of the oxidative flows of acetyl coenzyme A (CoA). Additionally, although the extent to which BHB is used by different brain cell types *in vivo* is unknown, tissue culture studies of neonatal and embryonic mouse cortex (Lopes-Cardozo et al., 1986) have reported that 60% of the BHB consumed in neurons is used for oxidation, whereas this is only 20% in astrocytes. Furthermore, measuring carbon dioxide (CO_2) production in units of umol substrate/mg protein/h, their data estimate approximately 70% of neuronal CO_2 production is from acetoacetate, whereas in astrocytes this figure is 40%, with much of the glial utilization based in membrane and lipid synthesis. Thus, BHB oxidation may be more reflective of neuronal metabolism. In this report, we describe the first use of [2,4-$^{13}C_2$]-β-hydroxybutyrate ([2,4-$^{13}C_2$]-BHB) to determine the properties of BHB transport and its oxidative contribution to human brain metabolism under conditions of acute hyperketonemia. We use *in vivo* MR spectroscopy in humans to follow the ^{13}C label from intravenously infused [2,4-$^{13}C_2$]-BHB, appearing in the studied brain volume and into cerebral metabolic intermediates, including ^{13}C-4-glutamate (Glu4) and ^{13}C-4-glutamine (Gln4). We develop a model to describe BHB oxidation in order to determine the oxidative contribution from BHB in the neuronal and astrocytic compartments. The results support the view that in humans BHB is oxidized in the large neuronal pool to a larger extent than in the astrocytic, with the rate of oxidation limited by ketone transport in these acutely hyperketonemic studies.

MATERIALS AND METHODS

Magnetic resonance

A Bruker Biospec 2.1T human MR system and an 8.5 cm diameter ^{13}C (22.55 MHz) surface coil with 13-cm-diameter quadrature ^{1}H (89.64 MHz) decoupling coils were used for all studies. As previously described, a localized adiabatic ^{13}C–[^{1}H] polarization transfer sequence was used for detection of ^{13}C (Shen et al., 1999). Localization was achieved through three-dimensional ISIS selecting a 6 × 4 × 6-cc^3 volume in the occipital–parietal lobes. Additional localization was achieved with outer volume suppression. The delays of the sequence were optimized for detection of the amino acid methylene resonances. Broadband decoupling was achieved with WALTZ-16 (Shaka et al., 1983) at a peak radio frequency (RF) amplitude of approximately 350 Hz, giving a residual splitting of less than 1 Hz over the complete ^{13}C spectral bandwidth.

Data processing

Data were processed using internally written software (MATLAB 6.0, the Mathworks Inc., Natick, MA, U.S.A.). After zero filling to 16 K and Gaussian broadening by 0.3 Hz, baseline correction was performed using a spline fit. Example of the correction is shown in Figure 1A. Resonances analyzed included ^{13}C-2-BHB (BHB2), ^{13}C-3-NAA (NAA3), ^{13}C-3-Asp (Asp3), ^{13}C-4-Glu (Glu4), ^{13}C-4-Gln (Gln4), ^{13}C-3-Glu (Glu3), ^{13}C-3-Gln (Gln3), ^{13}C-6-NAA (NAA6), and ^{13}C-4-BHB (BHB4). ^{13}C-3-Lactate (21.1 ppm) and ^{13}C-2,4-acetoacetate (30.1 and 54.0 ppm, respectively) were evaluated; however, no detectable labeling was seen at these positions. Before each labeling study, 60-min natural abundance (na) spectra were acquired from three of the four subjects. These were summed together to determine the ratios of resonances relative to $Glu4_{na}$. Thus, in all cases, the fractional enrichments were determined without assuming any specific concentrations of Glu, Gln, Asp, or NAA. On the day of the infusion study, 30-min natural abundance spectra were obtained from each subject immediately before the infusion to determine the $Glu4_{na}$ area. The peak areas of the other resonances M_{na} were thus scaled to $Glu4_{na}$. Curve fitting was performed with Gaussian lineshapes with the linewidths of the amino acids and NAA6 taken to be identical, and the two BHB resonances as identical. The labeling from the steady-state spectra, M_{ss}, was determined as a relative fractional enrichment (rFE) compared to natural abundance (M_{na}, known to be present at 1.1% concentration). Therefore, the rFE for metabolite M is given by $fM = 0.011 \cdot 100 \cdot (M_{ss} - M_{na})/M_{na}$. The relative fractional enrichment rFE is a percentage, and allows the direct comparison between different metabolites to interpret the pathways of labeling independent of concentration. For the BHB resonances (where no measurable natural abundance peaks were detected), the concentration was detected relative to the natural abundance NAA3 signal (NAA_{na}), taken at 10 mmol/L (Pan et al., 1998) according to $BHB = 0.011 \cdot 10 \cdot (BHB_{ss}/NAA_{na})$.

Physiology

All subjects were free of neurologic or psychiatric disorders. Under an Institutional Review Board–approved protocol, four adult subjects were studied. After an overnight fast, subjects were catheterized in the antecubital fossae bilaterally. One catheter was used for the infusion, the other for periodic blood sampling. After placement of catheters, the subject was positioned within the magnet, and acquisitions for system optimization were performed. After baseline MR data acquisition, the acute hyperketonemia was induced using a variant of the protocol earlier described (Pan et al., 2001). A sterile pyrogen-free solution of 200 mmol/L (pH 7.1) sodium [2,4-$^{13}C_2$]-D-BHB (100% fractional enrichment, Cambridge Isotope Laboratories) was infused at a bolus rate of 16.7 ml min^{-1} for 20 minutes, followed by 22 umol $\cdot kg^{-1} \cdot min^{-1}$ for the duration of the infusion study (approximately 120 minutes). During the study, samples were taken for glucose and lactate assays. Glucose assays were performed using a Beckman Glucometer (Beckman, Fullerton, CA, U.S.A.); lactate assays were performed using a YSI 2300 analyzer. Plasma BHB measurements were obtained offline using an Analox GM-7 analyzer and confirmed with 300-MHz high-resolution NMR studies (Bruker Avance, DRX-300). For the high-resolution studies, plasma samples were centrifuged through a Nanosept 10-K filter (Pall Life Sciences, Ann Arbor, MI, U.S.A.). Although the fractional enrichment of the plasma BHB was anticipated to be approximately 1.0, verification of this was provided through the high-resolution NMR studies.

RESULTS

Figure 1 shows a steady-state spectrum from volunteer 2, obtained from the final 60 minutes of a 2-hour infusion study. The steady-state plasma concentration of BHB in this volunteer was 2.18 mmol/L. The extent of baseline correction is shown. As is evident, the multiple

positions of glutamate, glutamine, and aspartate are well resolved. At the plasma ketone levels reached, the amount of dual labeling (^{13}C-3,4-glutamate) was negligible. The resonances of BHB are also well determined with the natural abundance peaks of NAA3 and NAA6. In all of these subjects, the BHB4 and NAA6 were easily resolvable, allowing two measurements (BHB2, BHB4) of the tissue BHB content.

Figure 2A shows the plasma and tissue BHB concentrations over the period of infusion from volunteer 4. The rise in plasma BHB is accompanied by a near simultaneous rise in the tissue levels, and reaches a steady state after 30 to 45 minutes of infusion. In 2 of the 4 subjects there was a further increase in plasma BHB above levels of approximately 2 mmol/L, which is consistent with the observations of Balasse and Fery (1989), finding a decrease in the BHB extraction ratio by muscle with increasing plasma BHB. Figure 2B displays the relative fractional enrichment of Glu4, Gln4, and Asp3, showing that the labeling begins to level off at approximately 60 minutes. The steady-state data in the amino acids reported in these studies (Table 1) were acquired during the final 20 minutes of infusion, from 100 to 120 minutes.

The steady-state spectrum of Figure 1 may be compared with that acquired using [1-^{13}C]-glucose and [1-^{13}C]-acetate, as published earlier by Shen et al. (1999) and Lebon et al. (2002), respectively, and reproduced in Fig. 3. (The BHB spectrum of Fig. 1 is reprocessed to approximately match that of the line broadening used in the glucose spectrum.) It is important to note that the pattern of labeling is similar with the notable exceptions of the BHB2 and BHB4 resonances, the minimal ^{13}C–^{13}C sidebands to the Glu4 resonances, and the absence of any lactate labeling. The ^{13}C–^{13}C sidebands (which would result from two sequential turns of the TCA cycle both picking up labeled acetyl CoA, thereby giving doubly labeled [3,4-^{13}C]-glutamate) are not observable due to the low fractional labeling of the acetyl CoA pool (approximately 7%). With this 7% labeling of the acetyl CoA pool, the anticipated fractional enrichment of doubly labeled [3,4-^{13}C]-glutamate is one third below that of singly labeled natural abundance glutamate and would not be detectable. No lactate was detected, in either individual subjects or in the summed data from all subjects. Table 1 shows a summary of the steady-state data from the 4 subjects, including the plasma BHB concentrations, brain BHB concentrations, and the rFE of other metabolites. The rFE of Glu4 (fGlu4) was 6.78 ± 1.71%, of fGln4 5.68 ± 1.84, and of fAsp3 3.99 ± 0.57%. It is evident that the fGlu3 and fGln4 are close to that of fGlu4, reaching a ratio of 87 ± 10% and 83 ± 9%, respectively, whereas the rFE of Glu4 is consistently higher than that of Asp3. The mean ratio of fAsp3/fGlu4 was 62 ± 16%.

DISCUSSION

Concentration of β-hydroxybutyrate at steady state and implications for control of ketone oxidation

The concentration of steady-state tissue BHB achieved by this infusion protocol is 0.18 ± 0.04 mmol/L, consistent with that determined in earlier ^{1}H studies using nonlabeled D-BHB infusions (Pan et al., 2001), at approximately 0.2 mmol/L. Because the measured concentrations include contributions from brain and nonbrain components (vascular, CSF), this value is an upper bound to the brain BHB concentration. Using a CSF–blood partition factor of 0.15 (Lamers et al., 1987) for BHB, a nonbrain volume contribution of 10%, and assuming that the relaxation parameters and visibility of blood and CSF BHB were equivalent to that of brain, a lower bound of brain BHB concentration would be approximately 50% less, at 97 ± 27 umol/L. Due to the large gradient between plasma and brain ketone concentrations there is unlikely to be significant ketone reverse transport. Thus, with minimal reverse flow and the oxidation rates discussed further on, this argues for blood–brain barrier transport control of ketone oxidation in the nonfasted state.

Calculation of the fractional contributions of β-hydroxybutyrate to neuronal oxidation

Consistent with earlier work of Cremer (1971), the label from [2,4-$^{13}C_2$]-BHB readily appears in the amino acids glutamate, glutamine, and aspartate. The BHB flow will be reflected by the labeling of the acetyl CoA pool, which, in turn, is displayed through the interaction of the acetyl CoA pool with TCA cycle intermediates and amino acids. To specifically evaluate the fate of the BHB, we may therefore consider the model displayed in Fig. 4A. In this model, BHB consumption occurs first in neurons, entering the astrocytic compartment after passage through neuronal glutamate. The directionality of glutamate/glutamine cycling is defined as shown, where glutamine synthesis occurs only in astrocytes and glutaminase activity is solely neuronal. This directionality is based on extensive tissue culture data demonstrating the major localization of these enzymatic activities (Martinez-Hernandez et al., 1977; Aoki et al., 1991) and is consistent with recent *in vivo* data using [1-^{13}C]-glucose and [2-^{13}C]-acetate as tracers (Shen et al., 1999; Lebon et al., 2002).

We therefore consider the quantitative contributions of ketone body oxidation as a function of the fractional enrichments of [4-^{13}C]-glutamate (fGlu4) and [4-^{13}C]-glutamine (fGln4). In this analysis, it should be noted that the equations that follow do not rely on any specific rate of exchange V_x between glutamate and α-ketoglutarate, because V_x would be expected to influence the kinetics of glutamate labeling, rather than the steady-state level. Given that the metabolic behavior of neuronal and astrocytic glutamine can be reasonably described by a single pool (in both glucose and acetate infusion studies (Shen et al., 1999; Lebon et al., 2002), and given that the concentration of astrocytic glutamate Glu_a is small (0.7 ± 0.5 mmol/L [Lebon et al., 2002]) compared to neuronal glutamate Glu_n (7 mmol/L, as a mean of gray and white matter), we consider the ratio fGln/fGlu to be close to the value of $fGln_a$/$fGlu_n$.

In this model BHB enters the neuron first, entering astrocytic pools after metabolism into glutamate. Equation 1 then gives the value of $2V_{kb,n}/V_{ox,n}$ (for details, see Appendix, Eq. A3) where both the astrocytic and neuronal pools are at steady state ($V_{ox,n}$ describes the oxidative flux in neurons and V_{cyc} is the flux of neurotransmitter-linked efflux of neuronal glutamate).

$$\frac{2V_{kb,n}}{V_{ox,n}} = fGlu_n4\left[1+\frac{V_{cyc}}{V_{ox,n}}\left(1-\frac{fGln_a4}{fGlu_n4}\right)\right] \geq fGlu_n4 \quad (1)$$

The measured value of $fGln_a4/fGlu_n4$ is 0.83 ± 0.09; thus the fractional contribution of ketones to neuronal oxidation is at least equal to or larger than $fGlu_n4$. It is important to note that, with this measured $fGln_a4/fGlu_n4$ value, it is evident that the ratio $2V_{kb,n}/V_{ox,n}$ is not very sensitive to the value of $V_{cyc}/V_{ox,n,}$ and can be approximated with the value of $fGlu_n4$, at 0.068 ± 0.017 (Table 1). This suggests that, with the ketone label, $fGlu_n4$ directly reflects the fractional labeling of the acetyl CoA pool. Notably, inclusion of malic enzyme flux would be expected to have a relatively small effect on the value of $2V_{kb,n}$ (see Appendix A). Using a V_{cyc} rate of 0.32 ± 0.07 mmol kg^{-1} min^{-1} (Lebon et al., 2002) with a $V_{ox,n}$ value of 0.80 ± 0.10 mmol kg^{-1} min^{-1} (Mason et al., 1999), this calculates $2V_{kb,n}/V_{ox,n}$ at 0.072 ± 0.17 (7.2%) and $V_{kb,n}$ = 0.058 ± 0.014 mmol kg^{-1} min^{-1}.

Calculation of the fractional contributions of β-hydroxybutyrate to astrocytic oxidation

It is straightforward to incorporate into this model an analysis describing how enrichments of glutamate, glutamine, and astrocytic fluxes interrelate with oxidative astrocytic ketone flux (see Appendix, B3). Equation 2, expressing the ketone fraction of total oxidation in

astrocytes, shows that the ratio $2V_{kb,a}/V_{ox,a}$ is relatively sensitive to astrocytic fluxes. Values for these fluxes are not readily available; Estimates of these have been made, however: $V_{ox,a}$ at 0.14 ± 0.06 mmol kg^{-1} min^{-1} or 0.06 ± 0.02 mmol kg^{-1} min^{-1} (Lebon et al. [2002] and Shen et al. [1999], respectively), V_{cyc} 0.32 ± 0.07 mmol kg^{-1} min^{-1} (Lebon et al., 2002), and $V_{gs} = V_{cyc} + V_{eff}$ = 0.36 ± 0.07 mmol kg^{-1} min^{-1} (Shen et al., 1999), and these will be used further on.

$$\frac{2V_{kb,a}}{V_{ox,a}} = fGln_a 4\left[1+\frac{V_{cyc}}{V_{ox,a}}\left(\frac{V_{gs}}{V_{cyc}} - \frac{fGlu_n 4}{fGln_a 4}\right)\right] \quad (2)$$

These values result in fairly variable estimates of $2V_{kb,a}/V_{ox,a}$ but using the larger $V_{ox,a}$ value (i.e., giving the high estimate for astrocytic ketone contribution) gives a value of 4.8 ± 3.3% ($2V_{kb,a}$ of 0.0068 ± 0.0046 mmol kg^{-1} min^{-1}). This percentage, as the fraction of ketones towards oxidation, is independent of the actual oxidative flux in neuronal or astrocytic pools. Using the high estimate for astrocytic ketone contribution, calculation of the neuronal to astrocytic fraction of oxidation for each subject gives a ratio of at least 1.85 ± 0.93 (i.e., that ketone oxidation is preferred by the neuronal over astrocyte compartment by at least 1.85). Summing the neuronal and astrocytic contributions gives a total $2V_{kb}$ rate of 0.064 ± 0.017 mmol kg^{-1} min^{-1}. The significance of the lower contribution of BHB towards astrocytic oxidation may be decreased if astrocytes are less dependent on oxidation for energy production and more glycolytic. As described by Lopes-Cardozo et al. (1986), however, astrocytes and neurons are similar in the amount of lactate produced per glucose consumed, with glucose contributing a larger fraction to CO_2 production in astrocytes than in neurons.

Total oxidation and comparison to existing data

The total contribution towards oxidation from [2,4-$^{13}C_2$]-BHB in these studies ranges from 0.065 to 0.060 mmol kg^{-1} min^{-1} and is dominated by the neuronal component. However, with the large tissue volume studied, it is evident that these data represent metabolic processing from both white and gray matter. Although some reports have suggested that this region in the occipital–parietal lobe is close to 100% gray matter (Gruetter et al., 2001), as it is in rodents, imaging data from humans have clearly shown otherwise. Normalized to brain tissue only (excluding CSF), in healthy adults this region is approximately 67% gray matter, 33% white matter (Pan et al., 2000*b*). Thus, the measurement of $2V_{kb}$ of 0.064 ± 0.017 mmol kg^{-1} min^{-1} (a V_{kb} of 0.032 ± 0.009 mmol kg^{-1} min^{-1}) likely reflects a more rapid gray matter rate in conjunction with a slower white matter rate. If we extrapolate the proportion of gray and white matter TCA cycle rates from PET and MR measurements (Lebrun-Grandie et al., 1983; Pan et al., 2000*b*), this would result in gray and white matter BHB oxidative rates of approximately 0.082 mmol kg^{-1} min^{-1} and 0.027 mmol kg^{-1} min^{-1}, respectively.

These values may be compared with the data reported earlier by Hasselbalch et al. (1996). These studies used whole brain AV differences to determine the consumption of ketones, and PET with [^{18}F]deoxyglucose to determine glucose consumption under conditions of acute (BHB infusion-induced) hyperketonemia. Hasselbalch et al. reported that, after reaching ketone levels of 2.16 ± 0.42 mmol/L, whole brain BHB consumption increased from 1.11 ± 1.23 umol 100 g^{-1} min^{-1} to 5.6 ± 2.25 umol 100 g^{-1} min^{-1}, with acetoacetate rising from 0.00 ± 0.01 to 2.49 ± 4.17 umol 100 g^{-1} min^{-1}. Together, these consumption rates, summed at 8.1 ± 4.7 umol 100 g^{-1} min^{-1}, would predict that, in acute hyperketonemia, ketones contribute about 24 ± 14% of total cerebral ATP production. This rate should be compared to our V_{kb} rate of 3.2 ± 0.9 umol 100 g^{-1} min^{-1}, on the low edge of

the range, but in relative agreement with Hasselbalch et al. (1996). Although we infused only [2,4-$^{13}C_2$]-BHB in this study, all the detected labeling in this study must have arisen from the ketone label, whether generated from acetoacetate or BHB. Thus, the comparison of our measurements of oxidative ketone flow (from $2V_{kb}/V_{tca}$) with that of Hasselbalch should be compared with the summed AV difference measurements that include both ketone bodies.

The present data can also be compared to that reported by Kunnecke et al. (1993). In these studies, brain extracts were taken from pentobarbital anesthetized (30 mg/kg) rats after a 2-hour infusion with 80 umol kg^{-1} min^{-1} of either labeled BHB or glucose. In BHB-infused rats, the ratio of Gln/Glu labeling was significantly higher than that measured with glucose-infused rats, by about a factor of 2. This was interpreted to indicate that BHB is preferentially used by glia, clearly in contrast to the present data. Three possible considerations may explain this: anesthesia, tissue composition of the studied volume, and species differences. First, Kunnecke et al. used intraperitoneal injections of pentobarbital (30 mg/kg) for anesthesia. As has been described by Mans et al. (1981), this would be expected to significantly decrease brain glucose consumption disproportionately to ketones. Under such conditions, it is likely that glucose labeling of the acetyl CoA pool is depressed, together with decreased neurotransmitter cycling, resulting in decreased glutamine labeling. Second, it is possible that in the human studies the inclusion of significant fraction of white matter to the tissue volume could alter the ratios of glutamine/glutamate labeling. In this case, white matter would effectively dilute the amount of apparent neurotransmitter cycling and lower the relative glutamine labeling. However, this is unlikely to wholly account for the similarity of labeling by glucose or BHB because voxels of similar gray and white matter composition were used in our studies and those of Lebon et al. (2002) and Shen et al. (1999). Finally, it is possible that species differences exist in the extent of glucose and BHB consumption. There is some suggestion for this, given the greater extent to which human brain can oxidize BHB in comparison to rodents (Hasselbalch, 1996; Hawkins, 1986). Thus, the present finding of a high rate of glutamate and glutamine labeling with BHB infusions in human brain suggests that BHB is preferentially oxidized in the large neuronal metabolic pool.

Evidence for compartmentation of aspartate

Recent work has suggested that aspartate may be distributed among several cell compartments in the brain, as opposed to being primarily localized with the large glutamate pool (glutamatergic neurons). Using the assumption that aspartate is present within the neuronal pool, the predicted enrichment would be 6.34 ± 2.79% (see Appendix C). This is significantly different from the measured Asp3 of 3.99 ± 0.57%. This suggests that, within the compartments that consume BHB, aspartate and glutamate are not equally distributed. Given the aforementioned evidence that BHB is preferentially used in the large neuronal pool, this would thus imply that aspartate is not codistributed with glutamate in this large pool.

Two possibilities are that either aspartate is located primarily in astrocytes, or that aspartate is distributed in a distinct metabolic pool of neurons. In the former, if aspartate were primarily astrocytic, prediction of the fAsp3 labeling (see Appendix, Eq. C2, using previously reported values of V_{ana} = 0.04 ± 0.02 mmol kg^{-1} min^{-1} (Shen et al., 1999) and $V_{tca,a}$ = 0.14 ± 0.06 mmol kg^{-1} min^{-1} (Lebon et al., 2002) would give a value of 3.44 ± 0.88%, closer to the observed 3.99 ± 0.57%. The latter possibility, of a predominance of aspartate in GABAergic neurons has been suggested by the finding of Waagepetersen et al. (2000) that cultured cortical GABAergic neurons labeled with [^{13}C]glucose gave a higher fractional enrichment of aspartate in comparison to fumarate. In either case, the difference in Asp3 from the predicted glutamate labeling provides evidence for a noncoincident

distribution of these two critical metabolites. This observation is of interest because the interpretation of oxidative rates from ^{13}C-labeling studies using aspartate and glutamate can be altered depending on their mutual distribution. Future measurements performed at higher magnetic field strengths, in which measurements of GABA, aspartate labeling from BHB may be acquired, may help resolve the specific cellular components aspartate is distributed in.

CONCLUSIONS

In summary, this is the first study directly showing acute utilization of BHB in human brain. The concentration of tissue BHB is in agreement with earlier acute hyperketonemic (nonfasted) data, with concentrations of brain BHB quite low. At the plasma levels of 2.25 ± 0.24 mmol/L BHB, the appearance of the ^{13}C label into the brain and into the amino acid pools is rapid, reaching a steady state for Glu4 and Gln4 at fractional enrichments of 6.78 ± 1.71% and 5.64 ± 1.84%, respectively. The distribution of label resembles that of glucose, consistent with the view that BHB is metabolized primarily within the large neuronal compartment. Modeling the glutamate and glutamine steady-state fractional enrichments based on a single compartment gives oxidative rates of BHB of 0.032 ± 0.009 mmol kg^{-1} min^{-1} that are consistent with whole brain human brain measurements made earlier using AV difference methods. Analysis of aspartate labeling is consistent with the view that in these compartments of BHB consumption, aspartate and glutamate are not equally distributed. We anticipate that information gained from these BHB studies will contribute towards defining the extent of BHB accumulation and the metabolic contributions that are not glucose dependent, which may be helpful towards understanding and managing clinical situations where glucose is not readily available, for example, the ketogenic diet and hypoglycemia.

Acknowledgments

This work was supported by the Charles A. Dana Foundation (J.W.P.), NIH-RO1–40550 (J.W.P.), NIH-RO1-NS37527 (D.L.R., R.A.G.), DK-49230 (K.F.P., G.I.S.), and NIH-PO1-NS39092 (H.P.H.).

APPENDIX

Metabolic model of BHB labeling

In this model, [2,4-$^{13}C_2$]-BHB is assumed to enter through the large neuronal compartment. The oxidative flux of [2,4-$^{13}C_2$]-BHB ($V_{kb,n}$) brings the ^{13}C label into ^{13}C-2-acetyl CoA (^{13}C-AcCoA) where it enters into the TCA cycle. Label is then rapidly transferred from α-ketoglutarate into ^{13}C-4-glutamate through rapid transamination and through glutamate dehydrogenase. Throughout the labeling study, the tissue is assumed to be at steady state so that values of specific fluxes are constrained by mass action. Early in the labeling study, the appearance of label is a result of isotopic flux. Once isotopic steady state has been reached, the $V_{kb,n}$ is taken as unchanging, as are the pool sizes of AcCoA, ^{13}C-AcCoA, glutamate, Glu4, glutamine, and Gln4. For example, in the case of the steady-state labeling of Glu4, we anticipate that there is no further change in the fractional enrichment of Glu4 (i.e., $dfGlu_n4/dt = 0$). This metabolite has four fluxes entering ($V_{kn,n}$, V_{gln}) and exiting ($V_{ox,,n}$, V_{cyc}) and is expressed in Eq. A1

$$\frac{dGlu_n4}{dt}=0=2V_{kb,n}-\left(V_{ox,n}+V_{cyc}\right)fGlu_n4+V_{gln}fGln_n4 \quad \text{(A1)}$$

Similarly Eq. A2 expresses fGln4:.

$$\frac{dGlu_n4}{dt}=0=V_{ret}fGln_a4-V_{gln}fGln_n4 \tag{A2}$$

Because of the absence of anaplerosis in this neuronal pool, and taking the case where malic enzyme flux is negligible, mass action (i.e., conserving pool size) requires that $V_{ret} = V_{cyc}$; thus, rearranging Eq. A1 and A2 gives Eq. A3 as shown in the text:

$$\frac{2V_{kb,n}}{V_{ox,n}}=fGlu_n4\left[1+\frac{V_{cyc}}{V_{ox,n}}\left(1-\frac{fGln_a4}{fGlu_n4}\right)\right] \tag{A3}$$

However, if malic enzyme flux were included in this model, this would make $V_{ret} = gV_{cyc}$ where g is greater than 1, resulting in Eq. A3a.

$$\frac{2V_{kb,n}}{V_{ox,n}}=fGlu_n4\left[1+\frac{V_{cyc}}{V_{ox,n}}\left(1-g\frac{fGln_a4}{fGlu_n4}\right)\right] \tag{A3a}$$

Depending on the value of g, the inclusion of malic enzyme flux would have a relatively small effect on the value of 2Vk. For example, if V_{ret} were 30% larger than V_{cyc},V_{kbn} would be 0.052, rather than 0.058 as described in the text.

The astrocytic compartment is described similarly through Eqs. B1 to B3

$$\frac{dGlu_a4}{dt}=0=2V_{kb,a}-\left(V_{ox,a}+V_{ga}\right)fGlu_a4+V_{cyc}fGlu_n4 \tag{B1}$$

$$\frac{dGln_a4}{dt}=0=V_{gs}fGlu_a4-\left(V_{eff}-V_{ret}\right)fGln_a4 \tag{B2}$$

Mass action in the astrocyte glutamine pool requires that $V_{gs} = V_{eff} + V_{ret}$, thus $fGln_a4 = fGlu_a4$. Thus combining Eqs. B1 and B2 and rearranging gives B3 (Eq. 2 in the text):

$$2V_{kb,a}=fGln_a4\left[V_{ox,a}+V_{cyc}\left(\frac{V_{gs}}{V_{cyc}}-\frac{fGlu_n4}{fGln_a4}\right)\right] \tag{B3}$$

If we similarly include a flux for malic enzyme in the astrocytic pool, this would modify Eq. B3 to B3a where $V_{gs} = gV_{cyc}$ (i.e., that $g = (V_{cyc} + V_{eff} + V_{me,a})/V_{gs}$):

$$2V_{kb,a}=fGln_a4\left[V_{ox,a}+V_{cyc}\left(g-\frac{fGlu_n4}{fGln_a4}\right)\right] \tag{B3a}$$

Aspartate labeling

Given that aspartate is anticipated to be in rapid equilibrium with oxaloacetate through amino transferases as seen with glutamate and α-ketoglutarate (see Fig. 4b), a neuronal aspartate localization would result in Eq. C1

$$\frac{dAsp_n3}{dt}=\frac{V_{ox,n}}{2}\left(fGlu_n4+fGlu_n3\right)-V_{tca,n}fAsp_n3 \tag{C1}$$

i.e., at steady state

$$fAsp_n3=\frac{1}{2}\left(fGlu_n4+fGlu_n3\right) \tag{C1a}$$

Astrocytic localization of aspartate would give Eq. C2

$$\frac{dAsp_a3}{dt}=\frac{V_{ax,a}}{2}\left(fGln_a4+fGln_a3\right)-V_{tca,a}fAsp_a3 \tag{C2}$$

which with conservation of astrocytic oxaloacetate concentration requiring that $V_{ana} + V_{ox,a} = V_{tca,a}$ can be solved at steady state to Eq. C2a.

$$fAsp_a3=\frac{1}{2}\left(fGln_a4+fGln_a3\right)\left(1-\frac{V_{ana}}{V_{tca,a}}\right) \tag{C2a}$$

Using values previously reported of $V_{ana} = 0.04 \pm 0.02$ mmol kg^{-1} min^{-1} and $V_{tca,a} = 0.18 \pm 0.07$ mmol kg^{-1} min^{-1} (Shen et al., 1999; Lebon et al., 2002), gives $fAsp_a3$ to be 3.44 ± 0.88%, close to the measured value of 3.99 ± 0.57%.

REFERENCES

Aoki C, Kaneko T, Starr A, Pickel VM. Identification of mitochondrial and non-mitochondrial glutaminase within select neurons and glia of rat forebrain by electron microscopic immunocytochemistry. J Neurosci Res 1991;28:531–548. [PubMed: 1714509]

Balasse EO, Fery F. Ketone body production and disposal: effects of fasting, diabetes and exercise. Diabetes Metab Rev 1989;5:247–270. [PubMed: 2656155]

Blomqvist G, Thorell JO, Ingvar M, Grill V, Widen L, Stone-Elander S. Use of R-β-[1-^{11}C]-hydroxybutyrate in PET studies of regional cerebral uptake of ketone bodies in humans. Am J Physiol 1995;269:E948–959. [PubMed: 7491948]

Cremer JE. Incorporation of label from D-β-hydroxy[^{14}C] butyrate and [3-^{14}C]-acetoacetate into amino acids in rat brain *in vivo*. Biochem J 1971;122:135–138. [PubMed: 5117566]

Gjedde A, Crone C. Induction processes in blood-brain transfer of ketone bodies during starvation. Am J Physiol 1975;229:1165–1169. [PubMed: 1200135]

Gruetter R, Seaquist ER, Ugurbil K. A mathematical model of compartmentalized neurotransmitter metabolism in the human brain. Am J Physiol 2001;281:E100–112.

Hasselbalch SG, Knudsen GM, Jakobsen J, Hageman LP, Holm S, Paulson OB. Brain metabolism during short-term starvation in humans. J Cereb Blood Flow Metab 1994;14:125–131. [PubMed: 8263048]

Hasselbalch SG, Madsen PL, Hageman LP, Olsen K, Justesen N, Holm S, Paulson OB. Changes in cerebral blood flow and carbohydrate metabolism during acute hyperketonemia. Am J Physiol 1996;270:E756–751.

Hawkins RA, Mans AM, Davis DW. Regional ketone body utilization by rat brain in starvation and diabetes. Am J Physiol 1986;250:E169–178. [PubMed: 2937307]

Kunnecke B, Cerdan S, Seelig J. Cerebral metabolism of [1,2-$^{13}C_2$]-glucose and [U-$^{13}C_4$]-3-hydroxybutyrate in rat brain as detected by ^{13}C NMR spectroscopy. NMR Biomed 1993;6:264–277. [PubMed: 8105858]

Lamers KJ, Doesburg WH, Gabreels FJ, Romsom AC, Lemmens WA, Wevers RA, Renier WO. CSF concentrations and CSF/blood ratio of fuel-related components in children after prolonged fasting. Clinica Chimica Acta 1987;167:135–145.

Lebon V, Petersen KF, Cline GW, Shen J, Mason GF, Dufour S, Behar KL, Shulman GI, Rothman DL. Astroglial contribution to brain energy metabolism in humans revealed by ^{13}C NMR spectroscopy: elucidation of the dominant pathway for neurotransmitter glutamate repletion and measurement of astrocytic oxidative metabolism. J Neurosci. 2002 in press.

Lebrun-Grandie P, Baron JC, Soussaline F, Loch'h C, Sastre J, Bousser MG. Coupling between regional blood flow and oxygen utilization in the normal human brain. Arch Neurol 1983;40:230–236. [PubMed: 6600924]

Lopes-Cardozo M, Larsson OM, Schousboe A. Acetoacetate and glucose as lipid precursors and energy substrates in primary cultures of astrocytes and neurons from mouse cerebral cortex. J Neurochem 1986;46:773–778. [PubMed: 3081684]

Mans AM, Biebuyck JF, Hawkins RA. Regional brain utilization of ketone bodies in starvation and diabetes. J Cereb Blood Flow Metab 1981;1(suppl 1):S90–91.

Martinez-Hernandez A, Bell KP, Norenberg MD. Glutamine synthetase: glial localization in brain. Science 1977;195(4284):1356–1358. [PubMed: 14400]

Mason GF, Pan JW, Chu WJ, Newcomer BR, Zhang Y, Orr R, Hetherington HP. Measurement of the TCA cycle rate in human gray and white matter *in vivo* by ^{1}H-^{13}C MR spectroscopy at 4.1T. J Cereb Blood Flow Metab 1999;19:1179–1188. [PubMed: 10566964]

Nehlig A, Boyet S, DeVasconcelos AP. Autoradiographic measurement of local cerebral β-hydroxybutyrate uptake in the rat during postnatal development. Neurosci 1991;40:871–878.

Owen OE, Morgan AP, Kemp HG, Sullivan JM, Herrera MG, Cahill JF. Brain metabolism during fasting. J Clin Invest 1967;46:1589–1595. [PubMed: 6061736]

Pan JW, Twieg DB, Hetherington HP. Quantitative ^{1}H spectroscopic imaging at 4.1T using B1 mapping and CSF referencing. Magn Res Med 1998;40:254–258.

Pan JW, Rothman DL, Behar KL, Stein DT, Hetherington HP. Human brain β-hydroxybutyrate and lactate increase in fasting-induced ketosis. J Cereb Blood Flow Metab 2000a;20:1502–1507. [PubMed: 11043913]

Pan JW, Stein DT, Telan G, Lee JH, Shen J, Brown P, Cline G, Mason GF, Shulman GI, Rothman DL, Hetherington HP. Spectroscopic imaging of glutamate C4 turnover in human brain. Magn Res Med 2000b;44:673–679.

Pan JW, Telang FW, Lee JH, deGraaf RA, Rothman DL, Stein DT, Hetherington HP. Measurement of β-hydroxybutyrate in acute hyperketonemia in human brain. J Neurochem 2001;79:539–544. [PubMed: 11701757]

Pollay M, Stevens FA. Starvation-induced changes in transport of ketone bodies across the blood-brain barrier. J Neurosci Res 1980;5:163–172. [PubMed: 6772797]

Robinson AM, Williamson DH. Physiological role of ketone bodies as substrates and signals in mammalian tissues. Physiol Rev 1980;60:143–187. [PubMed: 6986618]

Rothman DL, Novotny EJ, Shulman GI, Howseman AM, Petroff OA, Mason G, Nixon T, Hanstock CC, Prichard JW, Shulman RG. 1H-[^{13}C] NMR measurements of [4-^{13}C]glutamate turnover in human brain. Proc Natl Acad Sci U S A 1992;89:9603–9606. [PubMed: 1409672]

Shaka AJ, Keeler J, Freeman R. Evaluation of a new broadband decoupling sequence: WALTZ-16. J Magn Res 1983;53:313–340.

Shen J, Petersen KF, Behar KL, Brown P, Nixon TW, Mason GF, Petroff O, Shulman GI, Shulman RG, Rothman DL. Determination of the rate of the glutamate/glutamine cycle in the human brain by in vivo ^{13}C NMR. Proc Natl Acad Sci U S A 1999;96:8235–8240. [PubMed: 10393978]

Waagepetersen HS, Sonnewald U, Larsson OM, Schousboe A. Compartmentation of TCA cycle metabolism in cultured neocortical neurons revealed by ^{13}C MR spectroscopy. Neurochem Int 2000;36:349–358. [PubMed: 10733002]

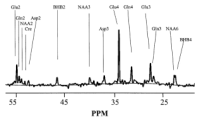

FIG. 1.

^{13}C spectrum, acquired from subject 2 during the 60- to 120-minute period in the infusion study. For processing parameters, see text.

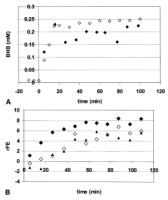

FIG. 2.

(A) Time course of brain (closed symbols) BHB in millimolar concentration. Open symbols are plasma BHB concentrations multiplied by 0.10. Data are from volunteer 4. The gradual increase in plasma BHB seen in this volunteer after plasma levels reached greater than 2 mmol/L was typical (see text). **(B)** Time course of the relative fractional enrichment of Glu4 (filled diamonds), Gln4 (open diamonds) and Asp3 (triangles) from volunteer 4.

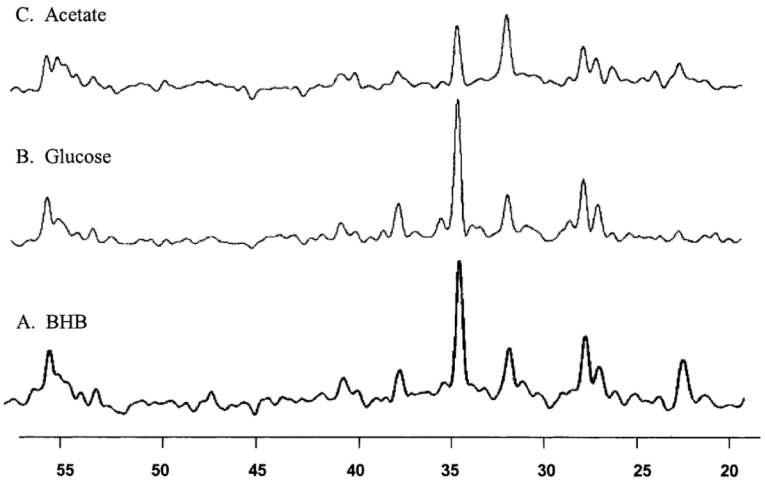

FIG. 3.

^{13}C spectra, acquired from infusions of BHB (**A**, bottom), glucose (**B**, middle), and acetate (**C**, top). The BHB spectrum was acquired during the 60- to 120-minute period in the infusion study (volunteer 2). For comparison between the three spectra, the BHB spectrum was processed using a Gaussian broadening of 1.8Hz. For processing parameters, see text. **(B)** ^{13}C spectrum acquired during the 120- to 160-min period in a ^{13}C-glucose infusion study, reproduced from Shen et al. (1999) **(C)** ^{13}C spectrum acquired during the 120- to 160-minute period in a ^{13}C-acetate infusion study.

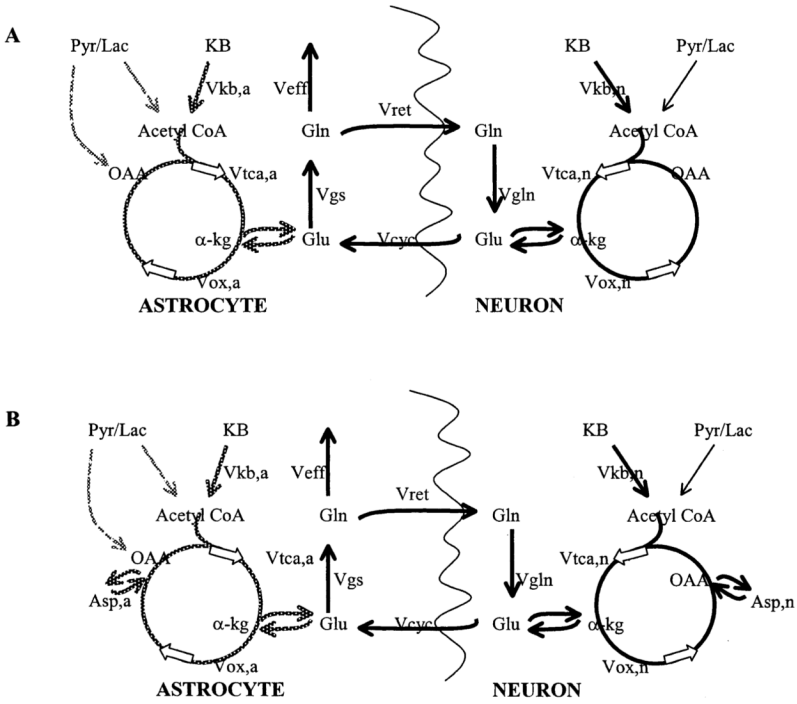

FIG. 4.

Metabolic model for BHB oxidation **(A)** showing flow in neurons and astrocytes. To distinguish between ketone flow from neuronal and astrocytic metabolism, the fluxes resulting from neuronal intake are shown in thick black; the fluxes resulting from astrocytic intake are in gray. **(B)** Model including flow into aspartate. KB, ketone body; Pyr/Lac, pyruvate + lactate; OAA, oxaloacetate; α-kg, α-ketoglutarate; Gln, glutamine; Glu, glutamate; Asp, aspartate; V_{kb}, oxidative flux of ketones either neuronal or astrocytic; V_{tca}, TCA-cycle rate flowing into α-kg, either neuronal or astrocytic; V_{ox}, TCA-cycle rate flowing out of α-kg, either neuronal or astrocytic; V_{cyc}, cycling rate between neuronal and astrocytic Glu; V_{gs}, glutamine synthesis rate; V_{ret}, return of astrocytic glutamine to neuronal glutamate; V_{gln}, neuronal glutaminase rate; V_{eff}, rate of loss of glutamine.

J Cereb Blood Flow Metab. Author manuscript; available in PMC 2010 December 1.

TABLE 1

Steady-state measurements: relative fractional enrichments, ratios, and concentrations

	rFE				Ratios of rFE			Concentration (mmol/L)	
Subject	**Glu4**	**Gln4**	**Glu3**	**Asp3**	**Gln4/Glu4**	**Glu3/Glu4**	**Asp3/Glu4**	**BHB (brain)**	**BHB (plasma)**
1	4.68	4.03	4.00	3.73	0.86	0.85	0.80	0.17	2.41
2	8.75	8.30	7.34	3.60	0.95	0.84	0.41	0.22	2.18
3	6.36	4.95	4.95	3.79	0.78	0.78	0.60	0.16	1.94
4	7.33	5.43	7.34	4.83	0.74	1.00	0.66	0.24	2.46
Mean	6.78	5.68	5.91	3.99	0.83	0.87	0.62	0.18	2.25
SD	1.71	1.84	1.70	0.57	0.09	0.10	0.16	0.06	0.24

rFE, relative fractional enrichments; glu, glutamate; glu, glutamine; asp, aspartate; BHB, [11C]- -hydroxybutyrate.